Chapter Five

Glucocorticoids modulate the mTOR pathway in the hippocampus: differential effects depending on stress history

J.A.E. Polman[1], R.G. Hunter[2], N. Speksnijder[1], J.M.E. van den Oever[1], O.B. Korobko[1], B.S. McEwen[2], E.R. de Kloet[1], N.A. Datson[1]

Endocrinology, September 2012, 153(9): 4317–4327

**J.A.E.P. and R.G.H. contributed equally to this work.*

[1] Division of Medical Pharmacology, Leiden/Amsterdam Center for Drug Research & Leiden University Medical Center, Leiden, the Netherlands
[2] Laboratory of Neuroendocrinology, The Rockefeller University, New York, USA

Glucocorticoid (GC) hormones, released by the adrenals in response to stress, are key regulators of neuronal plasticity. In the brain, the hippocampus is a major target of GC, with abundant expression of the GC receptor. GC differentially affect the hippocampal transcriptome and consequently neuronal plasticity in a subregion-specific manner, with consequences for hippocampal information flow and memory formation. Here, we show that GC directly affect the mammalian target of rapamycin (mTOR) signaling pathway, which plays a central role in translational control and has long-lasting effects on the plasticity of specific brain circuits. We demonstrate that regulators of the mTOR pathway, DNA damage-induced transcript (DDIT)4 and FK506-binding protein 51 are transcriptionally up-regulated by an acute GC challenge in the dentate gyrus (DG) subregion of the rat hippocampus, most likely via a GC-response element-driven mechanism. Furthermore, two other mTOR pathway members, the mTOR regulator DDIT4-like and the mTOR target DDIT3, are down-regulated by GC in the rat DG. Interestingly, the GC responsiveness of DDIT4 and DDIT3 was lost in animals with a recent history of chronic stress. Basal hippocampal mTOR protein levels were higher in animals exposed to chronic stress than in controls. Moreover, an acute GC challenge significantly reduced mTOR protein levels in the hippocampus of animals with a chronic stress history but not in unstressed controls. Based on these findings, we propose that direct regulation of the mTOR pathway by GC represents an important mechanism regulating neuronal plasticity in the rat DG, which changes after exposure to chronic stress.

5.1 Introduction

The hippocampus is a brain structure involved in cognitive processes and is a major target of glucocorticoid (GC) hormones, which are released by the adrenals in response to stress. Upon release, GC readily pass the blood-brain-barrier and target the GC receptor (GR), which is abundantly expressed throughout the brain and in particular in the hippocampus. GR is a ligand-inducible transcription factor and a member of the nuclear receptor family of transcription factors (Pratt, 1990). Due to its relatively low ligand affinity, most GR activation occurs at the circadian peak or during the stress response (Reul and de Kloet, 1985). Although nongenomic effects of GR exist (Johnson et al., 2005), GC effects on function and morphology of hippocampal neurons are to a large extent caused by transcriptional regulation of a wide repertoire of genes that play a central role in plasticity, energy metabolism, response to oxidative stress, and survival of hippocampal neurons (Magarinos et al., 1996; Tsolakidou et al., 2008).

GC are key regulators of neuronal plasticity and have profound effects on hippocampal function and viability. Hippocampal synaptic plasticity, a process fundamental to hippocampus-dependent learning and memory, is clearly affected by acute stress and concomitant GR activation and persists for hours after stress exposure (Howland and Wang, 2008; Kim et al., 2006). Acute stress and high concentrations of GC increase calcium current amplitude and impair long-term potentiation (LTP) in both hippocampal cornu ammonis (CA)1 and CA3 cell fields (Joels et al., 2003). Although the dentate gyrus (DG) region seems less sensitive to the effects of acute stress with respect to functional properties such as calcium current amplitude and α-amino-3-hydroxy-5-methyl-4-isoxazolepropionic acid (AMPA) receptor-mediated synaptic responses (Gemert Van et al., 2009; Joels et al., 2003), acute stress decreases new cell proliferation rate and increases apoptosis in the rat DG (Heine et al., 2004).

Like acute stress, chronic stress also affects hippocampal structure and function. Repeated stress causes remodeling of dendrites in the CA3 region (Magarinos et al., 1996; Sousa et al., 2000; Vyas et al., 2002; Watanabe et al., 1992). In the DG, chronic stress has effects on cell turnover of DG neurons and progenitor cells in the subgranular zone, where chronic stress suppresses both apoptosis and neurogenesis (Gould et al., 1997; Heine et al., 2004; Magarinos et al., 1996). After chronic stress exposure, synaptic excitation of DG cells may be enhanced when GC levels rise. This enhanced synaptic flow could contribute to enhanced excitation of projection areas of the DG, most notably the CA3 hippocampal region (Karst and Joels, 2003).

An important signaling pathway in the hippocampus is the mammalian target of rapamycin (mTOR) pathway, which plays a central role in translational control and long-lasting synaptic plasticity (Hoeffer and Klann, 2010). The mTOR pathway

integrates signals from nutrients, growth factors, and information on energy status to regulate many processes, including cell growth, cell proliferation, cell motility, and cell survival (Swiech et al., 2008; Wu et al., 2009). In neurons, the mTOR pathway modulates local translation of proteins at the synapse and therefore is critical for different forms of synaptic plasticity, including LTP and long-term depression (LTD) (Bekinschtein et al., 2007; Tang et al., 2002). Dysregulation of this pathway is a common hallmark in a wide variety of brain disorders, including autism, brain tumors, tuberous sclerosis, and neurodegenerative disorders, such as Parkinson's, Alzheimer's, and Huntington's disease (Akhavan et al., 2010; Bourgeron, 2009; Malagelada et al., 2008; Mozaffari et al., 2009; Pei and Hugon, 2008; Williams et al., 2008).

Although it is known that the mTOR pathway is subject to regulation by GC in the periphery (Shah et al., 2000c; Shah et al., 2000b; Wang et al., 2006a), so far little is known whether this also is the case in the brain. Two recent studies showed an inhibitory effect of GC on mTOR signaling in rat hypothalamic organotypic cultures and mouse cortical primary cultures (Howell et al., 2011; Shimizu et al., 2010), but to our knowledge, this has not been shown *in vivo* in the brain. In this study, we used an integrated genomics approach consisting of *in silico* predictions of GR binding sites, DNA microarrays, and chromatin immunoprecipitation (ChIP), to investigate whether the mTOR pathway is regulated by GC *in vivo* in the hippocampus. Here, we present data demonstrating that key regulators of the mTOR pathway, DNA damage-induced transcript (DDIT)4 [also known as regulated in development and DNA damage responses (REDD)1], FK506-binding protein 51 (FKBP51), DDIT4-like (DDIT4L) [also known as REDD2], and mTOR target DDIT3 (also known as CCAAT-enhancer-binding proteins homologous protein 3 or CHOP are regulated by GC in the DG subregion of the hippocampus. Interestingly, the GC regulation of DDIT4 and DDIT3 transcription as well as hippocampal mTOR protein levels after an acute GC challenge are differentially affected in animals previously exposed to chronic stress compared with controls. Based on these findings, we propose that direct regulation of the mTOR pathway by GC represents an important mechanism underlying GC effects on neuroplasticity in the brain, with different outcomes depending on previous stress history.

5.2 Materials and Methods

Experimental groups and collection of tissue

Animal experiments were performed to measure effects on the mTOR pathway at multiple levels, including DNA binding and effects on mRNA and protein levels. Because in the temporal sequence of events DNA binding precedes effects on transcription, which ultimately translate into effects at the protein level, different time

points were chosen depending on the parameter of interest. DNA binding was quantified at $t = 1\,\mathrm{h}$, mRNA changes at $t = 3\,\mathrm{h}$, and protein levels at $t = 5\,\mathrm{h}$.

For microarray analysis, male Sprague Dawley rats of $70\,\mathrm{d}$ of age (Charles River, Kingston, NY) were either handled for $21\,\mathrm{d}$ (control) or subjected to chronic restraint stress (CRS) for $6\,\mathrm{h}$ a d during $21\,\mathrm{d}$ (Hunter et al., 2009). On d 22, half of the rats received a challenge, which consisted of an injection with corticosterone (CORT) (sc $5\,\mathrm{mg/kg}$, in propylene glycol), and were killed $3\,\mathrm{h}$ later. The other half of the rats (control and CRS) were not challenged. Therefore, these rats were left undisturbed and did not receive a vehicle injection to avoid eliciting a stress response. The unchallenged rats were killed at the same time point as the injected rats. This resulted in four experimental groups (all $n = 6$) for the microarray analysis: 1) control, 2) control + CORT, 3) CRS, and 4) CRS + CORT. After decapitation, brains were rapidly dissected and snap frozen in isopentane (cooled in ethanol placed on pulverized dry ice) and stored at $-80\,^{\circ}\mathrm{C}$ for later use.

The experiment was repeated as described above ($n = 8$ per group) to determine effects of CRS and CORT challenge on mTOR protein levels using Western blot analysis, with the difference that the rats were killed $5\,\mathrm{h}$ after the CORT challenge on d 22. Hippocampi were immediately removed from the brain and processed for Western blot analysis (see below).

In a separate experiment, body weight and relative thymus weight were determined in control and CRS animals as a bioassay reflecting CORT exposure over the $21\,\mathrm{d}$ period. A clear decrease in body weight gain and relative thymus weight was observed upon CRS (Figure 5.6). Animal care was conducted in accordance with the Rockefeller University Animal Care Committee.

For ChIP analysis, male Sprague Dawley rats of $70\,\mathrm{d}$ of age (Harlan, Horst, The Netherlands) were adrenalectomized (ADX) as described before to completely deplete endogenous CORT levels and ensure that there was no GR bound to the DNA (Sarabdjitsingh et al., 2010a). Three days after ADX, one group of animals received an ip injection with $3\,\mathrm{mg/kg}$ CORT-hydroxypropyl-cyclodextrin complex, whereas the other group was left undisturbed ($n = 6$ per group). All animals were decapitated after $1\,\mathrm{h}$ for ChIP. Immediately after decapitation, the hippocampi were isolated and further processed for ChIP (see below). CORT levels in the blood $2\,\mathrm{d}$ after ADX and at the moment of decapitation were measured by RIA, showing that both the ADX operation was successful as well as a significant increase in CORT $3\,\mathrm{h}$ after injection (data not shown). Experiments were approved by the Local Committee for Animal Health, Ethics, and Research of the University of Leiden (Dier Experimenten Commissie nos. 06055 and 10044). Animal care was conducted in accordance with the European Commission Council Directive of November 1986 (86/609/EEC).

Microarray analysis

CA3 and DG subregions were isolated by laser microdissection from coronal brain sections ($8\,\mu\mathrm{m}$) containing the rostral rat hippocampus as previously described

(Datson et al., 2004). RNA was isolated using TRIzol (Invitrogen, Carlsbad, CA), linearly amplified for two rounds, and hybridized to Rat Genome 230 2.0 Arrays (Affymetrix, Santa Clara, CA) containing 31,099 probe sets representing over 28,000 well-substantiated rat genes. Hybridizations were conducted at the Leiden Genome Technology Center (Leiden University), according to the manufacturer's recommendations (Affymetrix). MAS 5.0 normalization of microarray data was performed in BRB-Array Tools version 3.7.0, an integrated package for the visualization and statistical analysis of DNA microarray gene expression data that operates as an add-in to Microsoft Excel (Simon et al., 2007). Normalized data were subsequently subjected to statistical analysis using Linear Models for Microarray Data (Smyth, 2005), a package for the R computing environment that allows multiple comparison of experimental groups. Differences in gene expression between groups were evaluated using two-way ANOVA with group and treatment as factors, followed by pairwise *post hoc* comparisons. Genes with $P \leq 0.05$ were considered significant. An extensive list of mTOR pathway members was assembled based on literature and checked for representation on the Affymetrix Rat Genome 230 2.0 Array.

Chromatin immunoprecipitation

Immediately after decapitation, the hippocampal tissue was chopped into pieces of approximately $1\,\mathrm{mm}$ and fixed in $1\,\%$ formaldehyde for 15 min under continuous rotation. Cross-linking was stopped by adding 0.125 M glycine for $5\,\mathrm{min}$. Subsequently, the tissue was washed three times with PBS and once with PBS containing protease inhibitors (PI). Pellets were snap frozen and stored at $-80\,^{\circ}\mathrm{C}$.

Defrosted pellets were homogenized for 2×10 sec in $0.5\,\mathrm{ml}$ of mild lysis buffer [$10\,\mathrm{mm}$ Tris-HCl (pH 7.5), $10\,\mathrm{mm}$ NaCl, and $0.2\,\%$ Nonidet P-40] supplemented with PI using the Bio-Gen PRO200 homogenizer. After centrifugation, the pellets were dissolved in $0.6\,\mathrm{ml}$ of PI-containing radioimmunoprecipitation assay buffer [$0.1\,\%$ sodium dodecyl sulfate, $1\,\%$ deoxycholate, $150\,\mathrm{mm}$ NaCL, $10\,\mathrm{mm}$ Tris (pH 8.0), $2\,\mathrm{mm}$ EDTA, $1\,\mathrm{mm}$ $NaVO_3$, $1\,\%$ Nonidet P-40, β-glycerolphophate, and Na-butyrate] and incubated on ice for 30 min. Subsequently, the chromatin was sheared (20 pulses of 30 sec., $200\,\mathrm{W}$; Bioruptor, Diagenode, Liège, Belgium), resulting in chromatin fragments of 100–$500\,\mathrm{bp}$, and stored at $-80\,^{\circ}\mathrm{C}$.

Sepharose A beads (GE Healthcare, Princeton, NJ) were blocked with $1\,\mathrm{mg/ml}$ bovine serum albumin (Westburg, Leusden, The Netherlands) and $0.2\,\mathrm{mg/ml}$ fish sperm (Roche Applied Science, Basel, Switzerland) for $1\,\mathrm{h}$ at $4\,^{\circ}\mathrm{C}$. Two ChIPs each were performed on the same batch of hippocampal chromatin derived from three different animals. Per ChIP, the chromatin was precleared by incubation with blocked beads for $1\,\mathrm{h}$. After preclearing, an input sample was taken to control for the amount of DNA used as input for the ChIP procedure. The remaining sample was divided into two samples, each incubated overnight (O/N) at $4\,^{\circ}\mathrm{C}$ under continuous rotation with either $6\,\mu\mathrm{g}$ of GR-specific H300 or normal rabbit IgG (Santa Cruz Biotechnology, Inc., Santa Cruz, CA). Subsequently, the antibody-bound DNA

fragments were isolated by incubating the samples with blocked protein A beads for 1 h at 4 °C. The beads were washed five times in 1 ml of washing buffer (1× low salt, 1× high salt, 1× LiCl, and 2× Tris-EDTA), followed by incubation with 0.25 ml of elution buffer (0.1 M $NaHCO_3$ and 1 % sodium dodecyl sulfate) for 15 min (room temperature, continuous rotation) to isolate the DNA-protein complexes. To reverse cross-link the DNA-protein interactions, the samples were incubated O/N at 65 °C with 0.37 M NaCl. RNAse treatment (0.5 µg/250 µl) was performed for 1 h at 37 °C followed by purification of DNA fragments on Nucleospin columns (Macherey-Nagel, Düren, Germany). The immunoprecipitated samples were eluted in 50 µl of elution buffer.

Western blot analysis

Hippocampal tissue was homogenized in radioimmunoprecipitation assay buffer with PI (04693124001; Roche Applied Science). Total protein concentration was measured by bicinchoninic acid assay according to the manufacturer's protocol (no. 23225, BCA Assay kit; Thermo Scientific, Rockford, IL). Electrophoresis of 20 µg of protein per sample was performed on a precast 4–20 % gradient gel (no. 456–1096; Bio-Rad Laboratories, Inc., Hercules, CA) and transferred O/N at 4 °C to Immobilon-P Transfer membrane (Millipore Corp., Billerica, MA). Primary antibody for mTOR (no. 2972; Cell Signaling Technology, Beverly, MA) was diluted 1:5000 and incubated O/N at 4 °C. Secondary antibody (goat antirabbit IgG horseradish peroxidase, no. 2054; Santa Cruz Biotechnology, Inc.) was incubated for 1 h at room temperature. Blots were exposed to ECL Hyperfilm (Amersham Biosciences, Buckinghamshire, UK) for 30 sec and scanned using an Epson V350 photo scanner (Epson, Long Beach, CA). Protein levels were quantified using ImageJ version 1.42. Signals were normalized against α-tubulin. Two-way ANOVA with group and treatment as factors was used to determine whether there were any significant differences, followed by pairwise *post hoc*comparisons. Significance was accepted at $P \leq 0.05$.

In silico GC response element (GRE) prediction

GenSig, an *in silico* screening method that uses a position weight matrix based on 44 published GREs, was used to identify evolutionary conserved GREs in the coding regions and a region 50 kb up- and downstream of the DDIT3 and DDIT4L genes (Simon et al., 2007; Datson et al., 2011). For DDIT4 and FKBP51, we had previously identified GREs and shown that GR binds to these sequences *in vivo* in the hippocampus (Simon et al., 2007; Datson et al., 2011).

Real-time quantitative PCR (RT-qPCR)

RT-qPCR was performed to validate the microarray results for the selected mTOR signaling genes. For mRNA analysis, cDNA was synthesized from the same experi-

Probe Set ID	Gene Symbol	Gene Title	ANOVA P-value	Control + CORT FC	Control + CORT P-value	Stress + CORT FC	Stress + CORT P-value
1369590_a_at	*Ddit3*	DNA damage-inducible transcript 3	5.5E−03	0.6	2.2E−03	NS	NS
1368025_at	*Ddit4*	DNA damage-inducible transcript 4	NS	1.9	3.0E−02	NS	NS
1368013_at	*Ddit4l*	DNA damage-inducible transcript 4 like	1.9E−08	0.3	1.8E−07	0.4	8.4E−06
1380611_at	*Fkbp5*	FK506-binding protein 5	8.6E−06	2.0	1.3E−04	2.0	1.7E−04
1388901_at	*Fkbp5*	FK506-binding protein 5	8.0E−11	2.0	5.0E−09	2.0	1.4E−08

Table 5.1: CORT regulation of the mTOR-associated transcripts.
CORT regulation of the mTOR-associated transcripts DDIT4, FKBP51, DDIT4L, and DDIT3 is indicated in control animals (*left*) and in animals with a recent history of CRS (*right*). The fold change (FC) is shown, in which *numbers* above 1 indicate an up-regulation and below 1 a down-regulation by acute CORT. $P > 0.05$ is considered not to be significant (NS).

mental RNA samples that were used for microarray analysis, using the iScript cDNA synthesis kit (Bio-Rad Laboratories, Inc.), according to manufacturer's instructions. PCR was conducted using the capillary-based LightCycler thermocycler and LightCycler FastStart DNA MasterPLUS SYBR Green I kit (Roche Applied Science) according to manufacturer's instructions. All PCR reactions on cDNA were performed in duplo, and obtained threshold cycle values were all between 12 (Tubulin beta-2A chain) and 19–25 (mTOR signaling genes). The standard curve method was used to quantify the expression differences (Smyth, 2005). cDNA values were normalized against Tubb2a expression levels and analyzed with GraphPad Prism 5 (GraphPad Software, Inc., San Diego, CA). Two-way ANOVA with group and treatment as factors was used in combination with *post hoc* testing to assess significant differential expression of GC-responsive genes. Significance was accepted at $P < 0.05$.

GR binding to predicted evolutionary conserved GREs in the vicinity of DDIT3, DDIT4, DDIT4L, and FKBP51 was validated using RT-qPCR on immunoprecipitated chromatin. All threshold cycle values ranged from 25 to 32. The ChIP PCR signal was normalized by subtracting the amount of nonspecific binding of the IgG antibody in the same sample. A further normalization for background noise was performed by subtracting the signal obtained at a nonbound GR region (exon 2 of the myoglobin gene). Metallothionein 2A, which has two well-documented GREs (Kelly et al., 1997), served as a positive control for the ChIP. Control genes metallothionein 2A and myoglobin were measured twice by RT-qPCR in both ChIPs. The hypothesized GREs were measured once per ChIP. Normalized data were analyzed with GraphPad Prism 5. An unpaired two-tailed t test was used to assess significant GR binding. Significance was accepted at a $P < 0.05$.

The primer sequences for microarray and ChIP validation are listed in Table 5.2.

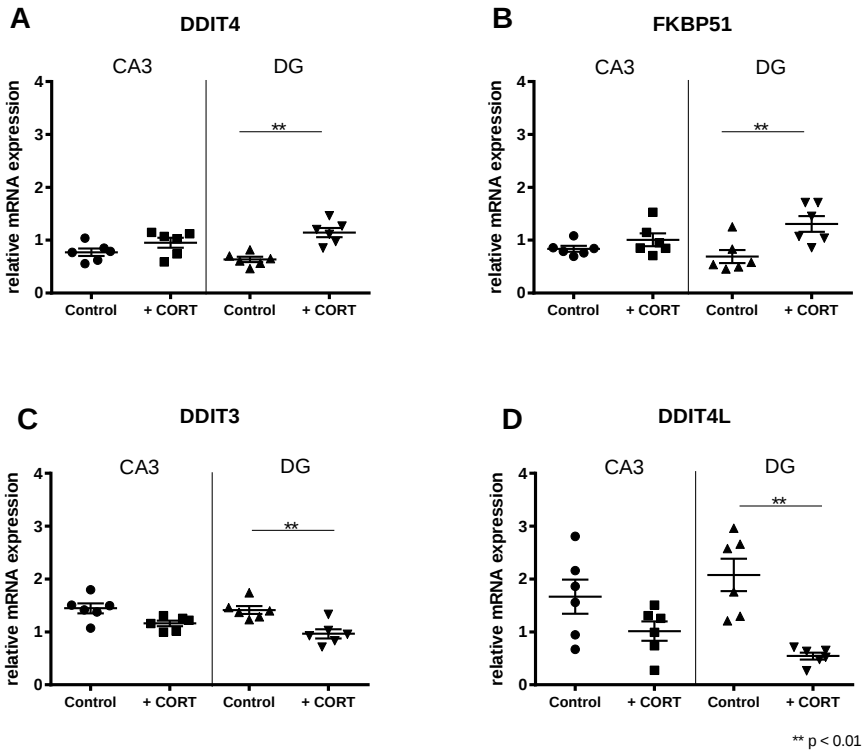

Figure 5.1: RT-qPCR validation of expression levels in control animals before and after GC challenge for DDIT4 (A), FKBP51 (B), DDIT3 (C), and DDIT4L (D).
RT-qPCR expression values were normalized against TUBB2a. *Each point in the graph* represents the expression of one animal. *Asterisks* indicate statistical significance: *, $P < 0.05$; **, $P < 0.01$.

5.3 Results

GC affect the expression of mTOR regulators in the hippocampus

Microarray analysis of mRNA expression in the rat hippocampal DG revealed differential expression of several mTOR regulators (FKBP51, DDIT4, and DDIT4L) and the mTOR target DDIT3 3 h after a CORT injection (Table 5.1). Both DDIT4 and FKBP51 were significantly up-regulated in the DG, whereas DDIT3 and DDIT4L were down-regulated. RT-qPCR confirmed the subregional differences in GC responsiveness of three out of four mTOR-associated transcripts (Figure 5.1).

According to the microarray analysis, none of these mTOR regulators were significantly affected by CORT in the CA3 region of the hippocampus at the applied

threshold of significance. However, according to RT-qPCR, DDIT3 was also GC responsive in CA3 ($P = 0.026$), albeit to a lesser extent than in the DG.

mRNA expression of mTOR itself and of other mTOR regulators such as v-akt thymoma viral proto-oncogene 1, tuberous sclerosis protein 1 and 2, regulatory associated protein of mTOR, rapamycin-insensitive companion of mTOR, and phosphatidylinositol 3 kinase were not differentially expressed in either the DG or the CA3 subregion of the hippocampus according to microarray analysis. A total of four other mTOR pathway members were expressed at significantly different levels between the groups according to ANOVA, of which two were differentially expressed in response to GC challenge both in control and in CRS animals: ribosomal protein S6 kinase polypeptide 2 and insulin receptor (Table 5.3).

FKBP51 and DDIT4 are primary targets of the GR in rat hippocampus

Using a position weight matrix based on 44 published GREs, we previously identified and confirmed GR binding to three evolutionary conserved GREs in the FKBP51 gene and a GRE 20 kb upstream of DDIT4 (Table 5.4) (Simon et al., 2007; Datson et al., 2011). Here, we replicated this finding in an independent experiment and confirmed GR binding to FKBP51_1 (one of the three GREs for FKBP51 that we selected) and the GRE near DDIT4 (Figure 5.2). Based on the GR binding to the GREs and their CORT-induced up-regulation, we conclude that FKBP51 and DDIT4 are primary targets of GR*in vivo* in the rat hippocampus and are most likely regulated by the transactivation mode of action of GR induced by GR-GRE interaction (Datson et al., 2011; Simon et al., 2007).

We used the same approach to screen for GREs in the vicinity of DDIT3 and DDIT4L, resulting in the identification of evolutionary conserved GRE-like sequences at 2,586 bp (DDIT3) and 2,199 bp (DDIT4L) downstream of the transcription start site of both genes (Table 5.4). However, we did not find GR binding to these predicted GREs associated with DDIT3 and DDIT4L under the given conditions.

GC effects on the mTOR pathway are modulated by previous chronic stress exposure

Because chronic stress is known to affect hippocampal synaptic plasticity, we were interested whether having experienced chronic stress shortly before receiving a CORT challenge would affect the pattern of GC regulation of the mTOR regulators and target. Interestingly, in animals with a previous history of CRS, the GC regulation of DDIT4 and DDIT3 in the DG was lost, whereas that of FKBP51 and DDIT4L was maintained (Table 5.1 and Figure 5.3). According to the microarray data, no GC regulation of any of the mTOR-associated genes was observed in the CA3 region in the CRS rats (data not shown).

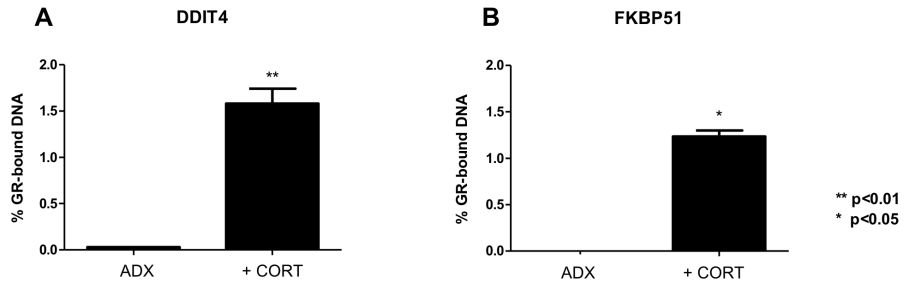

Figure 5.2: GR binding to the *in silico* predicted GREs in total hippocampus at 60 min after an ip injection of 3 mg/kg CORT.
GR binding is shown to the GRE associated with (A) DDIT4 and (B) FKBP51. The y-axis shows the percentage of input DNA that was bound by the GR. *Columns* represent average binding of two independent ChIP experiments each containing brain tissue of three different animals. The *error bars* equal sem. *Asterisks*indicate statistical significance: *, $P < 0.05$; **, $P < 0.01$.

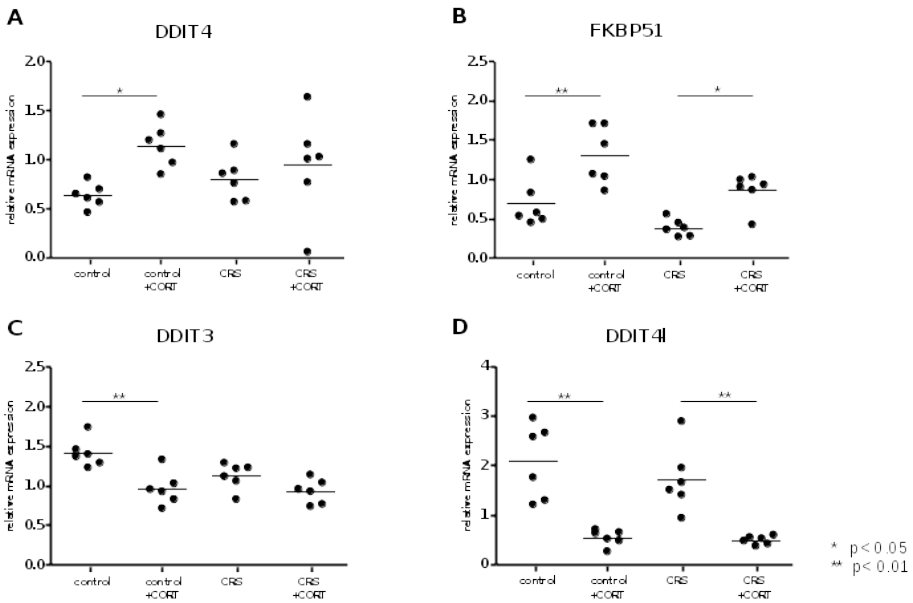

Figure 5.3: RT-qPCR indicating expression levels of DDIT4 (A), FKBP51 (B), DDIT3 (C), and DDIT4L (D) with and without an acute GC challenge in control animals and animals with a previous history of stress.
The GC responsiveness of DDIT3 and DDIT4 is lost in animals previously exposed to chronic stress. RT-qPCR expression values were normalized against TUBB2a. *Each point in the graph* represents the expression of one animal. *Asterisks*indicate statistical significance: *, $P < 0.05$; **, $P < 0.01$.

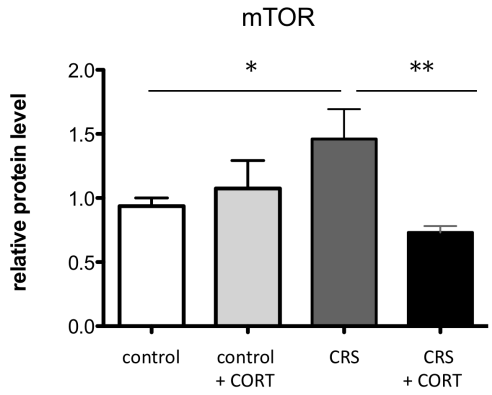

Figure 5.4: mTOR protein levels in the hippocampus measured by Western blotting.
mTOR protein levels were normalized against α-tubulin expression levels. Two-way ANOVA indicated that CORT had a significant effect on mTOR $F(1, 28)\ 4.200$; $P = 0.050$. In addition, there was a strong group-treatment interaction $[F(1, 28)\ 11.667; P = 0.002]$, indicating that CORT has significantly different effects on hippocampal mTOR protein levels in control and stress animals. *Asterisks* indicate statistical significance: *, $P < 0.05$; **, $P < 0.01$.

Hippocampal mTOR protein levels are differentially affected by acute GR activation depending on previous stress history

Based on the observation that in CRS animals, the GC regulation of DDIT4 and DDIT3 in the DG was lost, we were curious to determine the overall effect this would have on mTOR protein levels. Therefore, we quantified basal mTOR protein levels and levels $5\,\mathrm{h}$ after GR activation by an acute GC injection in control and CRS rats (Figure 5.4). Data were subjected to a two-way ANOVA with the factors group: control and CRS treatment, no treatment, and CORT. In addition, a *post hoc* test was applied to identify statistical significance between the four conditions. CORT had a significant effect on hippocampal mTOR protein levels [main effect of treatment, $F(1, 28)\ 4.200; P = 0.050$]. In addition, there was a significant group-treatment interaction $[F(1, 28)\ 11.667; P = 0.002]$, indicating that the CORT challenge had significantly different effects on hippocampal mTOR protein levels in control and CRS groups. In other words, giving an acute GC challenge had no effect on mTOR protein levels in the hippocampus of control animals ($P = 0.559$). However, in animals with a previous history of stress, an acute GC challenge resulted in a significant reduction in hippocampal mTOR protein ($P = 0.004$) (Figure 5.4). Without treatment, the stress group had significantly higher mTOR levels than the control group ($P = 0.032$).

5.4 Discussion

Here, we show that regulators of the mTOR pathway are targets of GC stress hormones in the hippocampal DG and to a lesser extent in CA3 pyramidal neurons. Furthermore, we demonstrate that the action of GC on the expression of mTOR pathway members as well as on hippocampal mTOR protein levels is context dependent and is highly sensitive to chronic stress.

GC as regulators of mTOR signaling in the brain

The mTOR pathway is a dynamically regulated system and has many upstream regulators that confer information from the extracellular environment to the cell. So far, not much is known on the extracellular signals that lead to mTOR activation in the brain. Several neuronal surface receptors, including N-methyl-D-aspartate receptors, dopaminergic, and metabotropic glutamate receptors as well as brain-derived neurotrophic factor, implicated in induction and maintenance of LTP and LTD, are known to influence mTOR function upon activation (Hoeffer and Klann, 2010). Although GC have been shown to repress mTOR signaling in several cell types, including lymphoid cells, skeletal muscle, hypothalamic organotypic cultures, and primary cortical neurons, to our knowledge, this has not been shown before *in vivo* in the brain (Howell et al., 2011; Shimizu et al., 2010; Wang et al., 2006a; Yan et al., 2006).

One of the proteins that is regulated by GC in the hippocampus is DDIT4 (or REDD1), which is known to inhibit mTOR activity, resulting in an increase in apoptosis in mouse embryonic fibroblasts (Corradetti et al., 2005; Ellisen et al., 2002). DDIT4L (or REDD2), which is approximately $50\,\%$ homologous to DDIT4, has also been found to inhibit mTOR signaling after GC stimulation in human embryonic kidney 293 and Chinese hamster ovary cells (Corradetti et al., 2005). This indicates that DDIT4 and DDIT4L are able to reduce cell proliferation and plasticity by inhibiting mTOR-mediated synthesis of proteins.

FKBP51 acts as a scaffolding protein decreasing v-akt thymoma viral proto-oncogene 1 functioning, resulting in decreased mTOR signaling and increased cell death (Pei et al., 2009; Pei et al., 2010). Interestingly, FKBP51 is one of the cochaperones involved in the nuclear signaling of GR and plays a role in GR sensitivity and regulation of the hypothalamic-pituitary-adrenal axis. Polymorphisms in FKBP51 have been associated with differences in GR sensitivity and GC stress response (Binder, 2009; Schiene-Fischer and Yu, 2001; Vermeer et al., 2003). Variations in the gene have been associated with increased recurrence of depression and with rapid response to antidepressant treatment (Binder et al., 2004). In particular, alleles associated with enhanced expression of FKBP51 after GR activation may represent a risk factor for stress-related psychiatric disorders (Binder, 2009).

DDIT3 (or CCAAT-enhancer-binding proteins homologous protein 3 or CHOP3) is a proapoptotic transcription factor that responds to availability of key nutrients,

such as amino acids, glucose, and lipids, and to endoplasmatic reticulum stress. DDIT3 is regulated by the mTOR pathway as well as by the activating transcription factor family and affects the expression of cell survival and death pathways (Chen et al., 2010; Di Nardo A. et al., 2009; Oyadomari and Mori, 2004).

Here, we present data that imply a fundamental and essential role of GC in regulating the mTOR pathway in the hippocampus, by transcriptionally regulating several mTOR pathway members. The GC regulation of mTOR pathway members was more robust in the DG than in the CA3. The relative lack of GR expression in CA3 (Van Eekelen et al., 1987) may explain the difference in degree of GC regulation of the mTOR pathway between both subregions. However, differences in GR expression are only one of the many fundamental differences in molecular architecture between the different subregions of the hippocampus, as we and others have previously shown (Datson et al., 2004; Datson et al., 2008; Greene et al., 2009; Lein et al., 2004).

GC responsiveness of FKBP51 and DDIT4 occurs via GR binding to GRE

In line with our findings, DDIT4 and FKBP51 were previously reported to be GC responsive and to contain potential GREs in their vicinity (Paakinaho et al., 2010; So et al., 2007). DDIT4 was originally identified to be responsive to dexamethasone treatment in T-cell lymphoma cell lines and thymocytes (Wang et al., 2003). Because treatment of these cells with the GR antagonist RU486 inhibited the induction of DDIT4, regulation via GR seemed likely. Indeed, in a ChIP-sequencing study, in which A549 cells (human lung adenocarcinoma epithelial cell line) were screened for GR-binding sites after dexamethasone stimulation, DDIT4 was found to be a primary GR target (So et al., 2007). Analysis of the GR-binding region revealed a GRE-like sequence, which is identical to the region that we have previously identified (Simon et al., 2007; Datson et al., 2011). Here, we demonstrate that DDIT4 is a primary target of the GR in the rat hippocampus.

In case of FKBP51, GREs surrounding the gene have also been studied extensively in A549 cells (Paakinaho et al., 2010). We recently predicted three evolutionary conserved GREs surrounding FKBP51 and showed that all three are bound by GR in the hippocampus (Simon et al., 2007; Datson et al., 2011). One of these (FKBP51_3) is a previously undescribed GRE and might be a specific GR target *in vivo* in the brain. This is of particular interest, given that polymorphisms in FKBP51 have been implicated as risk factors for several stress-related brain disorders, such as depression and posttraumatic stress disorder (Binder, 2009; Gillespie et al., 2009; Yehuda et al., 2009).

DDIT3 and DDIT4L are GC responsive but not GRE driven

DDIT3 and DDIT4L do not appear to be primary targets of GR in the rat brain, based on the fact that we did not find evidence of GR binding to the predicted GREs in the brain regions under the applied conditions. Consequently, we cannot fully exclude that these GREs might be bound by GR in a different time frame or in other tissues. However, given that both genes are down-regulated by GC in the DG, it seems more likely that they are regulated via the transrepression mode of action of GR, inhibiting the action of key transcription factors controlling DDIT3 and DDIT4L expression. Alternatively, they may be downstream secondary targets of GR, regulated by an intermediate GC-responsive transcription factor (Morsink et al., 2006a). DDIT3 is known to be a target of mTOR, but can also be regulated by the activating transcription factor family (Lein et al., 2004). Finally, a remote possibility is that the history of ADX has resulted in chromatin remodeling, shielding the GREs from GR binding. Chromatin remodeling has been postulated to occur as a consequence of GC pulsatility (Conway-Campbell et al., 2012) and aberrant GC exposure (Zhang et al., 2011).

What is the consequence of mTOR regulation by GC for the hippocampus?

In this study, we found opposing effects of GC injections on expression levels of mTOR regulators in control animals, *i.e*. up-regulation of DDIT4 and FKBP51 but down-regulation of DDIT4L, making it hard to predict *a priori* what the overall effect on mTOR protein levels would be. The opposing effects on mTOR regulators identified in the current study may represent a mechanism by which GC can fine-tune the overall outcome on mTOR signaling (Figure 5.5). A careful balance between mTOR inhibition and activation is essential to maintain neuronal health and function and prevent brain disease. For example, aberrant mTOR activation is a hallmark of brain tissue from rats with chronic seizures (Huang et al., 2010), but at the same time, mTOR is activated in the rat hippocampus during spatial learning (Qi et al., 2010) and is required for memory consolidation by controlling the increase of synaptic glutamate receptor 1 (Slipczuk et al., 2009).

Despite the GC-induced changes in expression of mTOR regulators in the DG after an acute challenge with GC, no change in mTOR protein was observed in the hippocampus of control animals, suggesting that a change in expression of mTOR regulators may be necessary to maintain the mTOR balance in the hippocampus.

Stress history changes GC responsiveness of the mTOR pathway

An interesting observation in this study is that chronic stress exposure had profound effects on the mTOR pathway. Chronic stress not only increased basal mTOR protein levels in the hippocampus but also abolished the GC responsiveness of

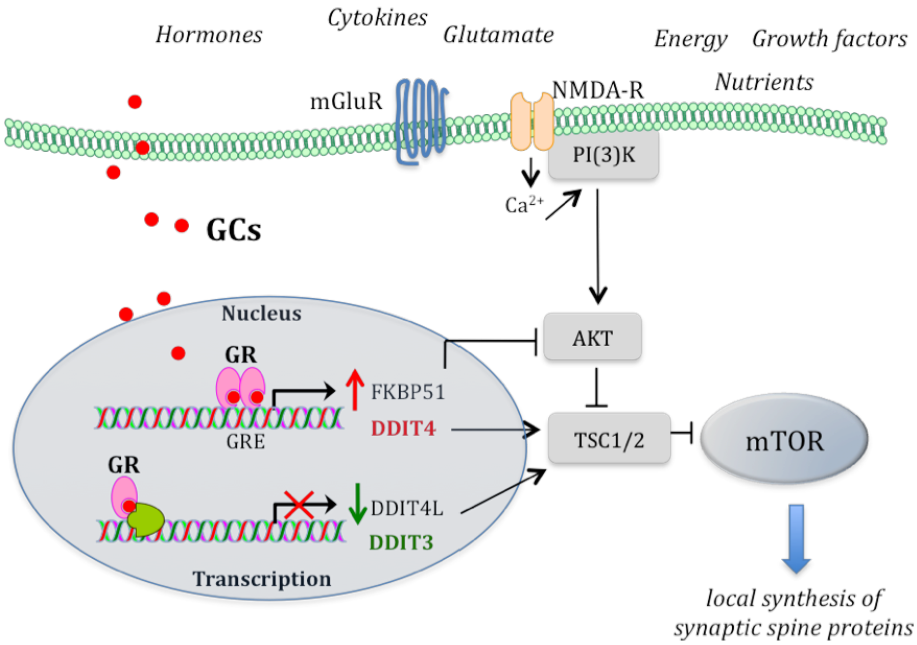

Figure 5.5: Schematic overview of key components of the mTOR pathway and a number of its physiological and molecular regulators in the brain, indicating a role for GC.
After GC binding to GR, FKBP51 and DDIT4 are up-regulated by a GRE-driven mechanism, whereas DDIT4L and DDIT3 are down-regulated via a non-GRE-driven mechanism. These mTOR regulators will influence the overall levels of mTOR, with consequences for local synthesis of synaptic spine proteins and thus for synaptic plasticity. PI3K, Phosphatidylinositol 3 kinase; AKT, v-akt thymoma viral protooncogene 1; NMDA-R, N-methyl-D-aspartate receptor; GluR, glutamate receptor; TSC1/2, tuberous sclerosis protein 1/2.

DDIT4 and DDIT3 in the DG. Moreover, an acute GC challenge was associated with a significant reduction in hippocampal mTOR protein levels.

Chronic stress has well-described effects on hippocampal structure and function, *i.e.* dendritic remodeling in CA3 (Magarinos et al., 1996; Sousa et al., 2000; Vyas et al., 2002; Watanabe et al., 1992) and suppression of apoptosis and neurogenesis in the DG (Gould et al., 1997; Heine et al., 2004; Magarinos et al., 1996). However, some of the changes in hippocampal function after chronic stress are not obvious under baseline conditions and only become apparent when GR is subsequently activated, such as the enhanced synaptic excitation of DG cells with respect to α-amino-3-hydroxy-5-methyl-4-isoxazolepropionic acid (AMPA) receptor-mediated synaptic responses in the DG (Karst and Joels, 2003). Local chromatin remodeling differentially affecting the transcriptional potential of individual genes and consequently the altered response to a subsequent GR activation may underlie both the enhanced synaptic excitability as well as the changes in GC regulation of mTOR pathway members in the DG after chronic stress. Indeed, CRS was recently shown to affect histone methylation patterns, resulting in changes in chromatin structure and conse-

quently changes in transcriptional potential (Hunter et al., 2009). These findings may explain why the GC responsiveness of DDIT4, a primary GR target driven by a classical GRE, is lost after CRS. For DDIT3, the mechanism is less clear, because we do not know whether it is a primary GR target via transrepression, a secondary target via an intermediate GC-responsive transcription factor, or a target gene of the mTOR pathway that is indirectly affected by GC. Future studies are required to elucidate the precise mechanism.

We hypothesize a model in which acute and chronic stress have differential effects on mTOR signaling, with consequences for LTP, LTD, and other neuroplastic processes as well as for survival/resilience pathways. In our model, control animals have a healthy mTOR balance, leading to efficient LTP and neuroprotection, which is not compromised by exposure to an acute GC challenge. Our data show that in animals exposed to chronic stress, hippocampal mTOR levels are increased, whereas if these animals are subjected to an additional stressor in the form of an acute GC challenge, mTOR levels are decreased. We therefore speculate that exposure to chronic stress results in a more dynamic mTOR balance, making it difficult to maintain a healthy equilibrium upon subsequent challenge and tipping the mTOR signaling balance toward a decrease in LTP and an increase in cell death pathways. Whether the effects of chronic stress on the mTOR balance signify greater vulnerability to damage or better adaptation is unclear. Future studies are required to test this model.

Interestingly, activation of the mTOR signaling pathway in the prefrontal cortex was recently shown to underlie the antidepressant action of ketamine, a nonselective N-methyl-D-aspartate receptor antagonist (Li et al., 2010). Fast activation of mTOR signaling by ketamine resulted in a rapid increase of synapse-associated proteins and spine number in the prefrontal cortex. Conversely, mTOR inhibition has been reported to have neuroprotective properties and to delay neurodegeneration (Choi et al., 2010; Spilman et al., 2010). GC may be important regulators of this delicate balance between mTOR activation and inhibition in the brain, with different effects depending on the context, timing, and exposure of neurons (Du et al., 2009). An optimal balance of the mTOR pathway would promote LTP and memory formation, while at the same time promoting cell survival and resilience. Indeed, chronic stress exposure suppresses LTP in the DG (Alfarez et al., 2003; Bodnoff et al., 1995; Krugers et al., 2006) and enhances vulnerability of DG granule cells to cell death (Gemert van et al., 2006).

5.5 Conclusion

The data presented here indicate that mTOR activity and the resulting translational processes it is involved in are regulated by GC in the rat brain. We show that GC regulate upstream mTOR regulators and that DDIT4 and FKBP51 are primary targets of GR in the hippocampus. Moreover, we demonstrate that the GC regulation of upstream mTOR regulators and downstream target DDIT3 differs between hippocampal subregions CA3 and DG, suggesting a key role of the mTOR pathway in the differential plasticity of these hippocampal subregions in response to acute GC exposure. Considering the fact that both GC and mTOR play an important role in neuroplasticity and neuronal survival (Bekinschtein et al., 2007; Swiech et al., 2008; Tang et al., 2002), we propose that GC play an important role in regulating the mTOR balance in the brain. Because GC regulation of mTOR regulators and mTOR protein levels is affected by a history of chronic stress, it would be of interest to further examine how these regulators are implicated in the pathogenesis of stress-related mental disorders.

Gene	mRNA Forward primer (5′–3′)	mRNA Reverse primer (3′–5′)	ChIP Forward primer (5′–3′)	ChIP Reverse primer (3′–5′)
Ddit3	CATGAACTGTTGGCATCACC	TGGAGATTACATGCTTGGCA	CCCCTTTCTCCACAGTGTTCCAGAA	AGCTGACTGGGAGGGTGGCTAA
Ddit4	TCTGAAAGGACCGAGCTTGT	ATAGCTGCCTCGAACAGGTC	CTGTGGGTGAGCTGAGAACA	GGCCTGTAGGTCCAGCACTA
Ddit4L	CACCCTGGGAGTCTGCTAAG	TTCAAACACCACCTCGTTGA	GGTGTTTGAAGAGACAACATGCCAGA	TGAGAGCCGCAGGACATCTTGG
FKBP5_1	AAGTGGCAAAGTGCCCAG	TCCAGGCTCAGGGTGTGAAGA	TCAGCACACCGAGTTCATGT	CTGGTCACTGCAAAACATCATT
MT2	AAGCTGCTGTTCCTGCTGCC	TTGTGAGGACGCCCCCACTTCA	AAAGTGATGCTTGGGCTGAG	AGGCAGGAAATGTGTTACCG
Myoglobin	AGCAGAGAACAGAAGAGGGGAGCA	AAGCAGAGGCCACTTTGCACCT	TAGTGTGCATCCAGCAGAGG	ACACTGTGGCCTTTTTGTCC

Table 5.2: Primer sequences for microarray and ChIP validation.

Probe Set ID	Gene Symbol	Gene Title	ANOVA P-value	Control + CORT FC	Control + CORT P-value	Stress + CORT FC	Stress + CORT P-value
1368862_at	Akt1	v-akt murine thymoma viral oncogene homolog 1	NS	NS	NS	NS	NS
1375178_at	Akt1	V-akt murine thymoma viral oncogene homolog 1	NS	NS	NS	NS	NS
1383126_at	Akt1	V-akt murine thymoma viral oncogene homolog 1	NS	NS	NS	NS	NS
1372879_at	Akt1s1	AKT1 substrate 1 (proline-rich)	NS	NS	NS	NS	NS
1375117_at	Akt1s1	AKT1 substrate 1 (proline-rich)	NS	NS	NS	NS	NS
1375766_at	Akt1s1	AKT1 substrate 1 (proline-rich)	NS	NS	NS	NS	NS
1368832_at	Akt2	v-akt murine thymoma viral oncogene homolog 2	NS	NS	NS	NS	NS
1378425_at	Akt2	v-akt murine thymoma viral oncogene homolog 2	NS	NS	NS	NS	NS
1387353_at	Akt2	V-akt murine thymoma viral oncogene homolog 2	NS	NS	NS	NS	NS
1388765_at	Akt2	V-akt murine thymoma viral oncogene homolog 2	NS	NS	NS	NS	NS
1372874_at	Akt3	v-akt murine thymoma viral oncogene homolog 3	NS	NS	NS	NS	NS
1387592_at	Akt3	v-akt murine thymoma viral oncogene homolog 3	NS	NS	NS	NS	NS
1373837_at	Aktip	AKT interacting protein	NS	NS	NS	NS	NS
1385103_at	Aktip	AKT interacting protein	NS	NS	NS	NS	NS
1372243_at	Cab39	calcium binding protein 39	NS	NS	NS	NS	NS
1372244_at	Cab39	calcium binding protein 39	NS	NS	NS	NS	NS
1383341_at	Cab39l	calcium binding protein 39-like	NS	NS	NS	NS	NS
1369590_a_at	Ddit3	DNA-damage inducible transcript 3	**5.5E−03**	**0.6**	**2.2E−03**	NS	NS
1368025_at	Ddit4	DNA-damage-inducible transcript 4	**9.1E−02**	**1.9**	**3.0E−02**	NS	NS
1368013_at	Ddit4l	DNA-damage-inducible transcript 4-like	**1.9E−08**	**0.3**	**1.8E−07**	**0.4**	**8.4E−06**

Probe Set ID	Symbol	Gene Title	ANOVA	Control + CORT		Stress + CORT	
1369621_s_at	Fkbp1a	FK506 binding protein 1a	NS	NS	NS	NS	NS
1398828_at	Fkbp1a	FK506 binding protein 1a	NS	NS	NS	NS	NS
1398829_at	Fkbp1a	FK506 binding protein 1a	NS	NS	NS	NS	NS
1380611_at	Fkbp51	FK506 binding protein 5	**8.6E−06**	**2.0**	**1.3E−04**	**2.0**	**1.7E−04**
1388901_at	Fkbp51	FK506 binding protein 5	**8.0E−11**	**2.0**	**5.0E−09**	**2.0**	**1.4E−08**
1371528_at	Fkbp8	FK506 binding protein 8	NS	NS	NS	NS	NS
1376070_at	Fkbp8	FK506 binding protein 8	NS	NS	NS	NS	NS
1371255_at	Hras	Harvey rat sarcoma virus oncogene	NS	NS	NS	NS	NS
1370333_a_at	Igf1	insulin-like growth factor 1	NS	NS	NS	NS	NS
1367652_at	Igfbp3	insulin-like growth factor binding protein 3	NS	NS	NS	NS	NS
1386881_at	Igfbp3	insulin-like growth factor binding protein 3	NS	NS	NS	NS	NS
1368424_at	Ikbkb	inhibitor of kappa light polypeptide gene enhancer in B-cells, kinase beta	NS	NS	NS	NS	NS
1397547_at	Ikbkb	Inhibitor of kappa light polypeptide gene enhancer in B-cells, kinase beta	NS	NS	NS	NS	NS
1369051_at	Insr	insulin receptor	NS	NS	NS	NS	NS
1392043_at	Insr	insulin receptor	**4.5E−03**	**0.8**	**2.4E−02**	**0.7**	**9.4E−03**
1369771_at	Irs1	insulin receptor substrate 1	NS	NS	NS	NS	NS
1369078_at	Mapk1	mitogen activated protein kinase 1	NS	NS	NS	NS	NS
1373426_at	Mapk1	mitogen activated protein kinase 1	NS	NS	NS	NS	NS
1398346_at	Mapk1	mitogen activated protein kinase 1	NS	NS	NS	NS	NS
1387771_a_at	Mapk3	mitogen activated protein kinase 3	NS	NS	NS	NS	NS
1389167_at	Mapkap1	mitogen-activated protein kinase associated protein 1	NS	NS	NS	NS	NS
1367963_at	Mlst8	MTOR associated protein, LST8 homolog (S. cerevisiae)	NS	NS	NS	NS	NS
1368019_at	Mtor	mechanistic target of rapamycin (serine/threonine kinase)	NS	NS	NS	NS	NS
1368079_at	Pdk1	pyruvate dehydrogenase kinase, isozyme 1	NS	NS	NS	NS	NS
1370052_at	Pdpk1	3-phosphoinositide dependent protein kinase-1	NS	NS	NS	NS	NS
1376795_at	Pik3ap1	phosphoinositide-3-kinase adaptor protein 1	NS	NS	NS	NS	NS
1378506_at	Pik3c2a	phosphoinositide-3-kinase, class 2, alpha polypeptide	NS	NS	NS	NS	NS
1379433_at	Pik3c2a	phosphoinositide-3-kinase, class 2, alpha polypeptide	NS	NS	NS	NS	NS
1381576_at	Pik3c2b	phosphoinositide-3-kinase, class 2, beta polypeptide	NS	NS	NS	NS	NS
1394770_at	Pik3c2b	phosphoinositide-3-kinase, class 2, beta polypeptide	NS	NS	NS	NS	NS
1369050_at	Pik3c2g	phosphoinositide-3-kinase, class 2, gamma polypeptide	NS	NS	NS	NS	NS
1369655_at	Pik3c3	phosphoinositide-3-kinase, class 3	NS	NS	NS	NS	NS

Probe Set ID	Symbol	Gene Title	ANOVA	Control + CORT		Stress + CORT	
1374232_at	Pik3ca	phosphoinositide-3-kinase, catalytic, alpha polypeptide	NS	NS	NS	NS	NS
1379041_at	Pik3ca	phosphoinositide-3-kinase, catalytic, alpha polypeptide	NS	NS	NS	NS	NS
1382366_at	Pik3ca	phosphoinositide-3-kinase, catalytic, alpha polypeptide	NS	NS	NS	NS	NS
1389143_at	Pik3ca	phosphoinositide-3-kinase, catalytic, alpha polypeptide	NS	NS	NS	NS	NS
1393499_at	Pik3ca	phosphoinositide-3-kinase, catalytic, alpha polypeptide	NS	NS	NS	NS	NS
1396411_at	Pik3ca	phosphoinositide-3-kinase, catalytic, alpha polypeptide	NS	NS	NS	NS	NS
1373528_at	Pik3cd	phosphoinositide-3-kinase, catalytic, delta polypeptide	NS	NS	NS	NS	NS
1393755_at	Pik3cd	phosphoinositide-3-kinase, catalytic, delta polypeptide	NS	NS	NS	NS	NS
1370114_a_at	Pik3r1	phosphoinositide-3-kinase, regulatory subunit 1 (alpha)	NS	NS	NS	NS	NS
1370100_at	Pik3r2	phosphoinositide-3-kinase, regulatory subunit 2 (beta)	NS	NS	NS	NS	NS
1376190_at	Pik3r2	phosphoinositide-3-kinase, regulatory subunit 2 (beta)	NS	NS	NS	NS	NS
1369518_at	Pik3r3	phosphoinositide-3-kinase, regulatory subunit 3 (gamma)	NS	NS	NS	NS	NS
1389723_at	Pik3r4	phosphoinositide-3-kinase, regulatory subunit 4	NS	NS	NS	NS	NS
1374317_at	Pik3r6	Phosphoinositide-3-kinase, regulatory subunit 6	**3.9E−02**	NS	NS	NS	**2.0E−02**
1370529_a_at	Pld1	phospholipase D1	NS	NS	NS	NS	NS
1370530_a_at	Pld1	phospholipase D1	NS	NS	NS	NS	NS
1370531_a_at	Pld1	phospholipase D1	NS	NS	NS	NS	NS
1370532_at	Pld1	phospholipase D1	NS	NS	NS	NS	NS
1370679_at	Pld1	phospholipase D1	NS	NS	NS	NS	NS
1368954_at	Pld2	phospholipase D2	NS	NS	NS	NS	NS
1387384_at	Pld2	phospholipase D2	NS	NS	NS	NS	NS
1369104_at	Prkaa1	protein kinase, AMP-activated, alpha 1 catalytic subunit	NS	NS	NS	NS	NS
1394921_at	Prkaa1	protein kinase, AMP-activated, alpha 1 catalytic subunit	NS	NS	NS	NS	NS
1369654_at	Prkaa2	protein kinase, AMP-activated, alpha 2 catalytic subunit	NS	NS	NS	NS	NS
1386945_a_at	Prkab1	protein kinase, AMP-activated, beta 1 non-catalytic subunit	NS	NS	NS	NS	NS
1369271_at	Prkab2	protein kinase, AMP-activated, beta 2 non-catalytic subunit	NS	NS	NS	NS	NS
1378845_at	Prkab2	Protein kinase, AMP-activated, beta 2 non-catalytic subunit	NS	NS	NS	NS	NS
1367947_at	Prkag1	protein kinase, AMP-activated, gamma 1 non-catalytic subunit	NS	NS	NS	NS	NS
1373952_at	Prkag2	protein kinase, AMP-activated, gamma 2 non-catalytic subunit	NS	NS	NS	NS	NS
1375835_at	Prkag2	Protein kinase, AMP-activated, gamma 2 non-catalytic subunit	NS	NS	NS	NS	NS
1383122_at	Prkag2	protein kinase, AMP-activated, gamma 2 non-catalytic subunit	NS	NS	NS	NS	NS
1392263_at	Prkag2	protein kinase, AMP-activated, gamma 2 non-catalytic subunit	NS	NS	NS	NS	NS

Probe Set ID	Symbol	Gene Title	ANOVA	Control + CORT		Stress + CORT	
1394711_at	Prkag3	protein kinase, AMP-activated, gamma 3 non-catalytic subunit	NS	NS	NS	NS	NS
1370112_at	Pten	phosphatase and tensin homolog	**4.2E−02**	NS	NS	NS	NS
1375360_at	Rheb	Ras homolog enriched in brain	NS	NS	NS	NS	NS
1398787_at	Rheb	Ras homolog enriched in brain	NS	NS	NS	NS	NS
1397877_at	Rictor	RPTOR independent companion of MTOR, complex 2	NS	NS	NS	NS	NS
1370261_at	Rps6ka1	ribosomal protein S6 kinase polypeptide 1	NS	NS	NS	NS	NS
1374811_at	Rps6ka2	ribosomal protein S6 kinase polypeptide 2	**3.4E−07**	**1.9**	**3.1E−06**	**1.7**	**5.2E−05**
1382271_at	Rps6ka5	ribosomal protein S6 kinase, polypeptide 5	NS	NS	NS	NS	NS
1398582_at	Rps6ka5	ribosomal protein S6 kinase, polypeptide 5	NS	NS	NS	NS	NS
1388646_at	Rptor	regulatory associated protein of MTOR, complex 1	NS	NS	NS	NS	NS
1367736_at	Rraga	Ras-related GTP binding A	NS	NS	NS	NS	NS
1369696_at	RragB	Ras-related GTP binding B	NS	NS	NS	NS	NS
1382719_at	RragB	Ras-related GTP binding B	NS	NS	NS	NS	NS
1371723_at	Rragc	Ras-related GTP binding C	NS	NS	NS	NS	NS
1382537_at	Rragc	Ras-related GTP binding C	NS	NS	NS	NS	NS
1373427_at	Rragd	Ras-related GTP binding D	NS	NS	NS	NS	NS
1375238_at	Stk11	Serine/threonine kinase 11	NS	NS	NS	NS	NS
1375364_at	Stk11	serine/threonine kinase 11	NS	NS	NS	NS	NS
1381830_x_at	Stk11	Serine/threonine kinase 11	NS	NS	NS	NS	NS
1375896_at	Stradb	STE20-related kinase adaptor beta	NS	NS	NS	NS	NS
1376476_at	Telo2	TEL2, telomere maintenance 2, homolog (S. cerevisiae)	NS	NS	NS	NS	NS
1394982_at	Telo2	TEL2, telomere maintenance 2, homolog (S. cerevisiae)	NS	NS	NS	NS	NS
1367830_a_at	Tp53	tumor protein p53	NS	NS	NS	NS	NS
1367831_at	Tp53	tumor protein p53	NS	NS	NS	NS	NS
1370752_a_at	Tp53	tumor protein p53	NS	NS	NS	NS	NS
1369362_at	Tsc1	tuberous sclerosis 1	NS	NS	NS	NS	NS
1368056_at	Tsc2	tuberous sclerosis 2	NS	NS	NS	NS	NS
1370168_at	Ywhaq	tyrosine 3-monooxygenase/tryptophan 5-monooxygenase activation protein, theta polypeptide	NS	NS	NS	NS	NS
1387862_at	Ywhaq	tyrosine 3-monooxygenase/tryptophan 5-monooxygenase activation protein, theta polypeptide	NS	NS	NS	NS	NS

Table 5.3: Microarray analysis of mRNA expression in the rat hippocampal DG in control animals (left) and in animals with a recent history of CRS (right). The fold change (FC) is shown, in which *numbers* above 1 indicate an up-regulation and below 1 a down-regulation by acute CORT. $P > 0.05$ is considered not to be significant (NS). NS: not significant ($p > 0.05$), FC: fold change

	Gene	GRE sequence	Distance from TSS
Ddit4	*Rattus Norvegicus*	*gaacattgtgttct*	−20,879
	Homo sapiens	gaacattgtgttct	−24,936
	Mus Musculus	gaacattgtgttct	−22,516
	Bos Taurus	gaacattgtgttct	−15,283
Ddit4L	*Rattus Norvegicus*	*gaactgtctgtcca*	2,199
	Homo sapiens	gaactgtctgtcca	2,382
	Mus Musculus	gaactgtctgtcca	2,324
	Bos Taurus	gaactgtctgtcca	2,557
Ddit3	*Rattus Norvegicus*	*ctccacagtgttcc*	2,586
	Homo sapiens	gcccacagtgttca	2,755
	Mus Musculus	ctccacagtgttcc	2,894
	Bos Taurus	ccccacagtgttcc	2,613
Fkbp51_1	*Rattus Norvegicus*	*gaacagggtgttct*	62,946
	Homo sapiens	gaacagggtgttct	86,842
	Mus Musculus	gaacagggtgttct	20,724
	Bos Taurus	gaacagggtgttct	99,485

Table 5.4: The in silico predicted GRE-sequences and their location relative to the transcription startsites in four different species. In case of DDIT4, DDIT4L and FKBP51_1, the sequence is 100 % conserved in all species.

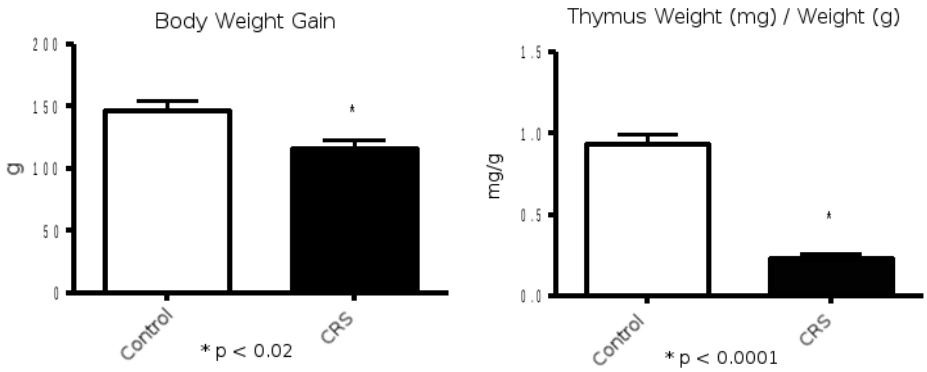

Figure 5.6: Body weight gain and relative thymus weight in control and CRS animals. Students test shows significant differences on both measures ($n = 8$ for both groups).